Supplementary File

Supplementary Figures Legends

Supplementary Figure S1. Many breakpoints concentrate to a narrow region on Chromosome 9. Scatter graphs of all CONAN reported breakpoints on the *p* arm of Chromosome 9. **A** Left breakpoint closer to the telomere of p arm. **B**. Right breakpoint closer to the centromere of *p* arm. Note that there is a concentration of breakpoints between coordinates 20,000,000 and 25,000,000.

Supplementary Figure S2. Distribution of CDKN2A homozygous deletions. Shown are all the deletions reported on COSMIC/CONAN from all sources. The skewness and kurtosis statistics are also shown.

Supplementary Figure S3. **The telomere proximal (left) breakpoints of homozygous deletions are concentrated in a narrower region than the centromere proximal (right) breakpoints. A**. X-Y scatter graph of the left and right breakpoints for all homozygous deletions that include the CDKN2A. X-axis shows the CDKN2A telomere proximal chromosomal coordinates and Y-axis the centromere proximal coordinates. The Pearson's correlation coefficient is =-.325 indicating that there is no correlation between the chromosomal coordinates of the telomere breakpoints and the centromere breakpoints. **B**. Graph showing the distribution of the homozygous deletions organized by the position of the telomere proximal breakpoint. **C**. Graph showing the distribution of the homozygous deletions organized by the position of the centromere proximal breakpoint.

Supplementary Figure S4. **Replication forks map in the telomere proximal CDKN2A region. A**. UCSC genome browser snapshot of the chromosome interval where the left breakpoint occurs. The picture shows transcriptional direction of some loci as well as histone H3K27Ac marks and DNA hypersensitivity peak clusters. **B**. OK-Seq data with similar chromosomal coordinates as in **A** indicating origins of replication from Petryk N et al. The red and blue dots represent Okazaki fragments. When read from left to right, an origin of replication is determined by a shift between blue and red dots. A termination or replication fork convergence site is represented by a shift between red and blue. Two origins of replication and a termination site are present in the region where a high level of breaks occur. **C**. Repetitive elements in the region between the two origins of replication as reported by UCSC genome browser. Shown are SINEs, LINEs and other short repeats as well as long segmental duplications. For the segmental duplications, the chromosomal duplications the left break point coordinates are given in base pairs.

Supplementary Figure S5. Distribution of homozygous deletion breakpoints for most commonly affected loci. Maps of all homozygous deletions for each of the indicated loci are shown. Each bar represents the span of the deletion between the two breakpoints. Skewness and kurtosis statistics are also shown. PTEN is reproduced here identically as in **Figure 5C** to allow visual comparison with the other genes.

Supplementary Figure S1. Many breakpoints concentrate in a narrow region on Chromosome 9

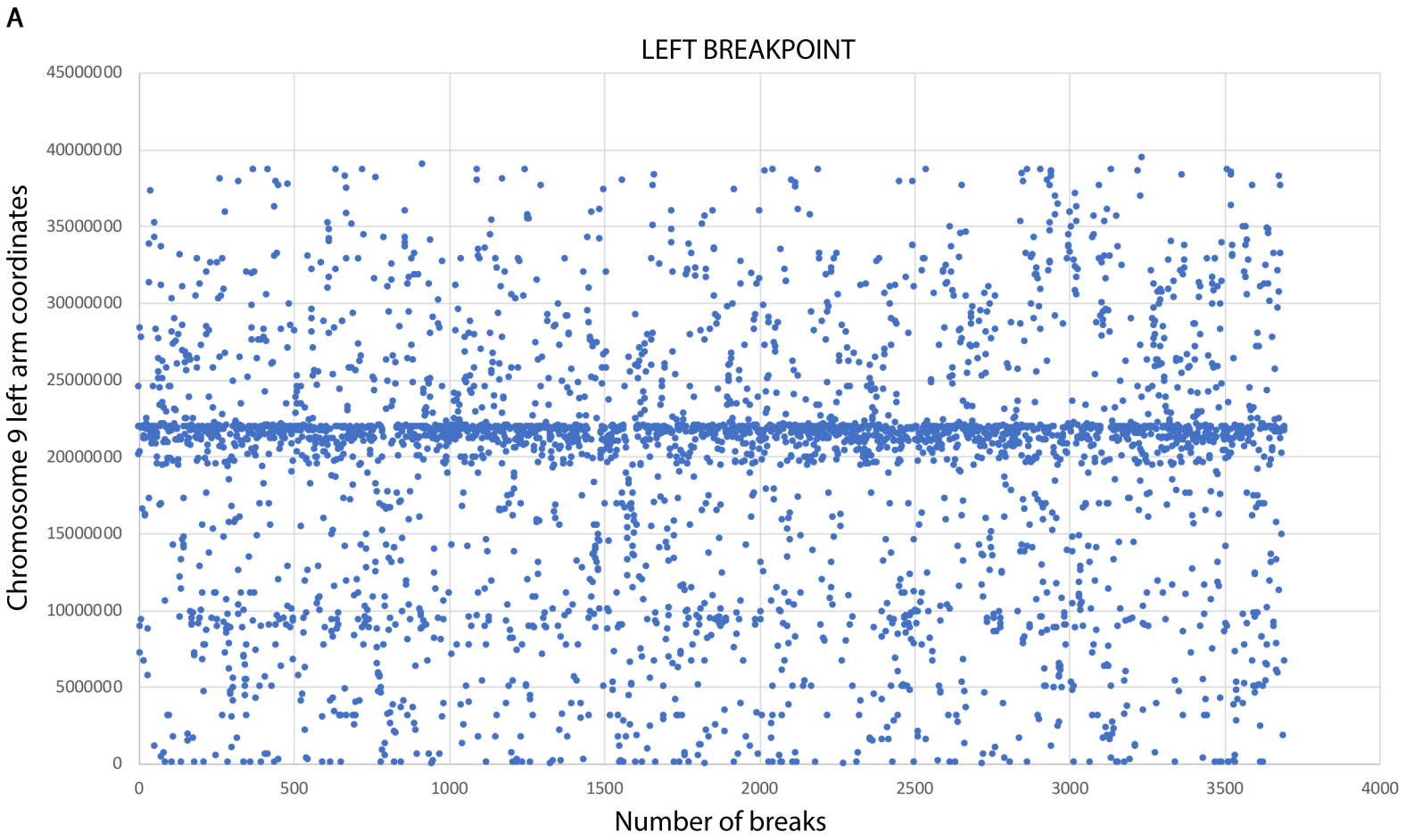

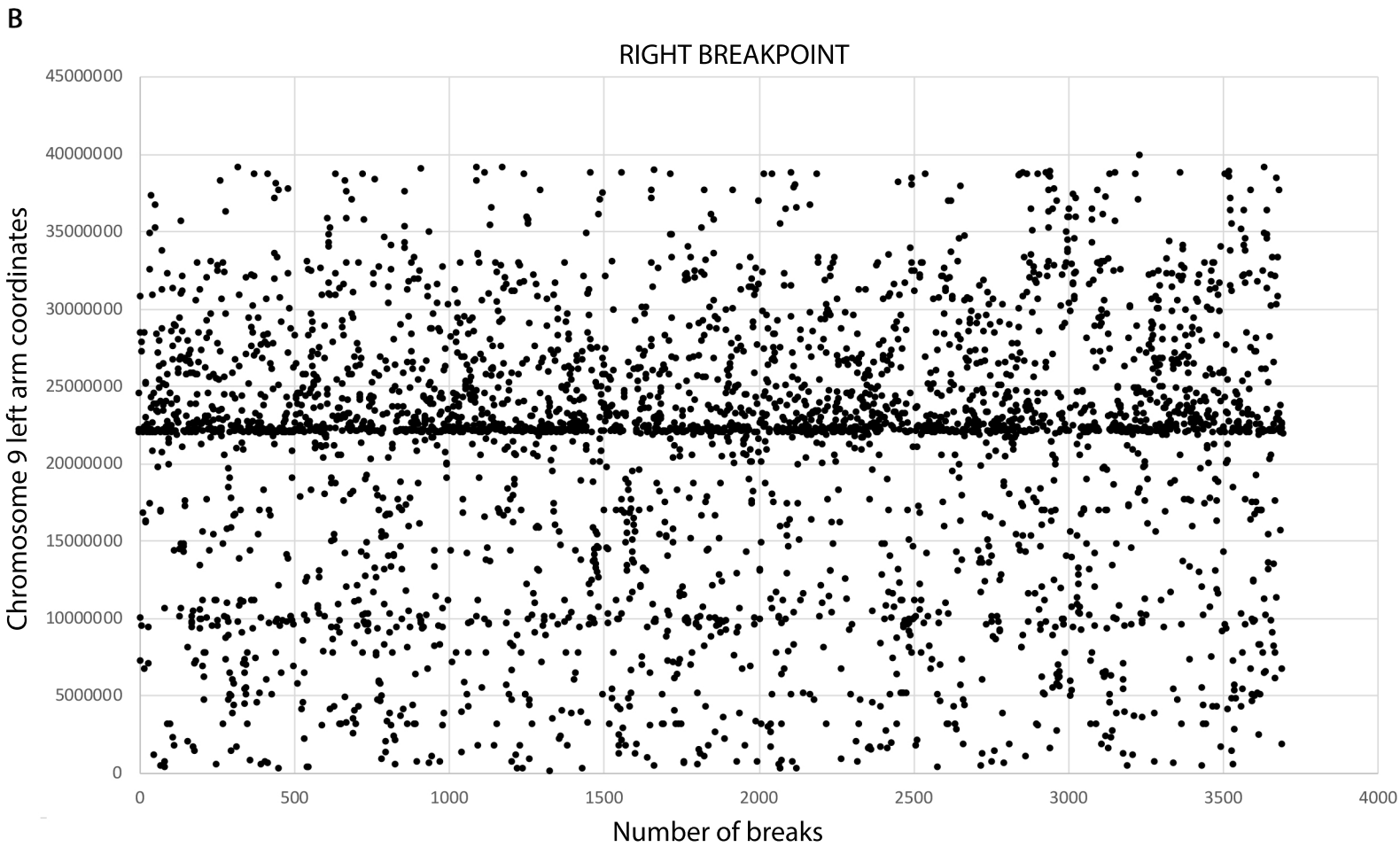

Supplementary Figure S2. Distribution of all CDKN2A homozygous deletions

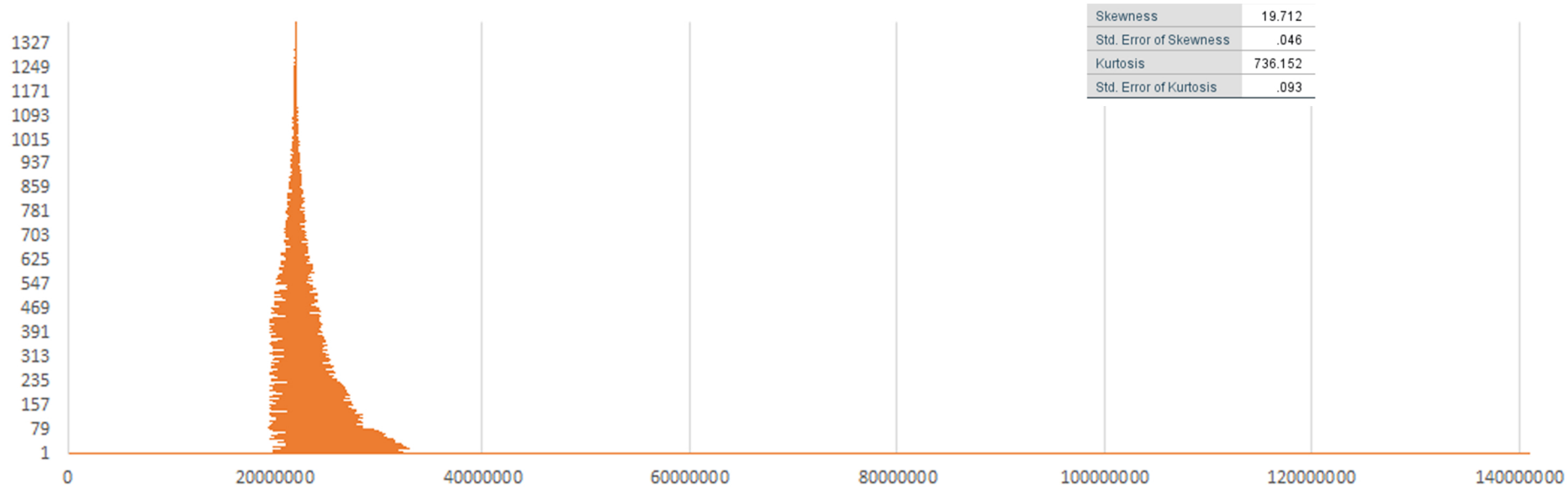

Supplementary Figure S3. The telomere proximal (left) breakpoints of homozygous deletions are concentrated in a narrower region than the centromere proximal (right) breakpoints.

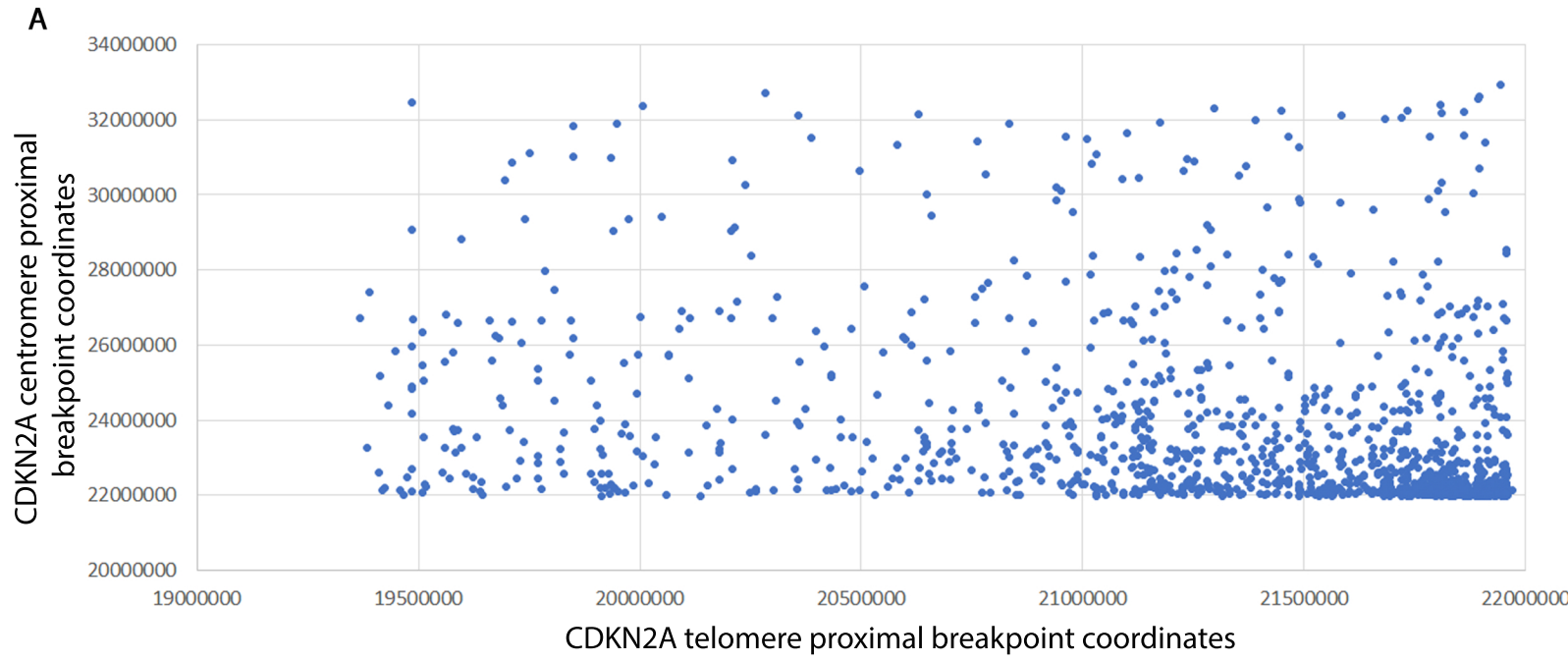

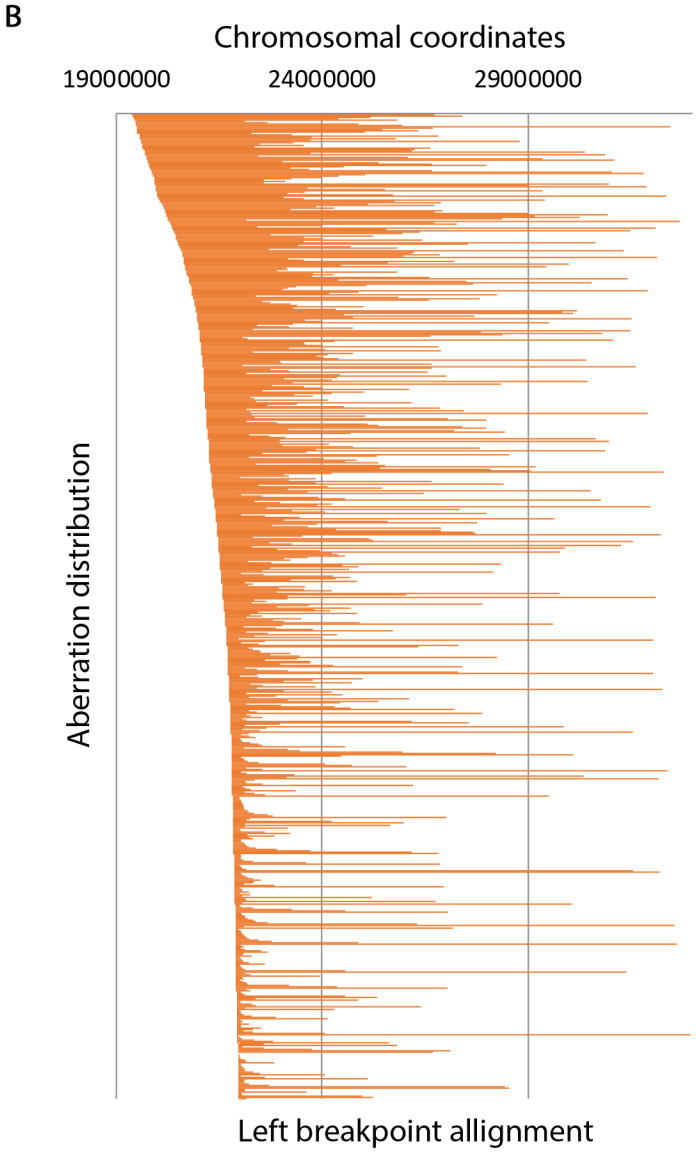

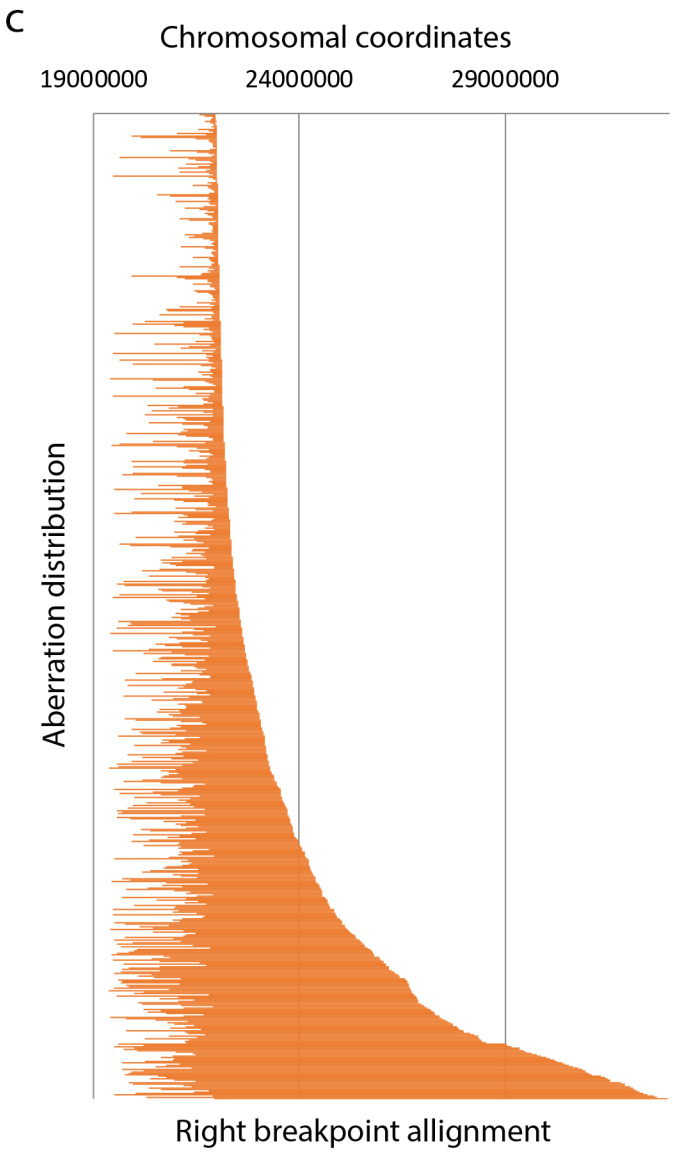

Supplementary Figure S4. Landscape of origins of replication in the CDKN2A telomere proximal region

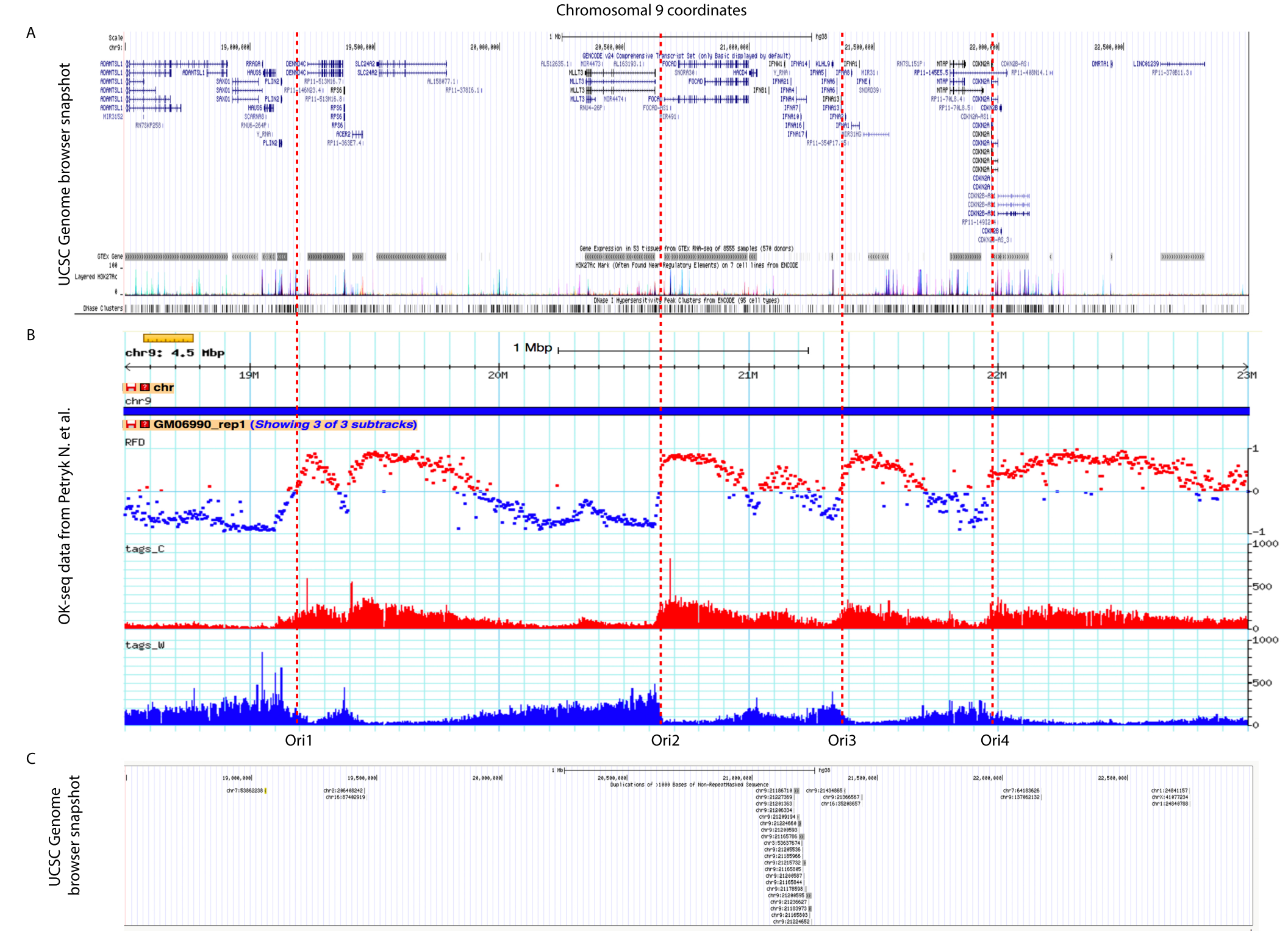

Supplementary Figure S5. Distribution of homozygous deletions breakpoints for most commonly affected loci

TP53

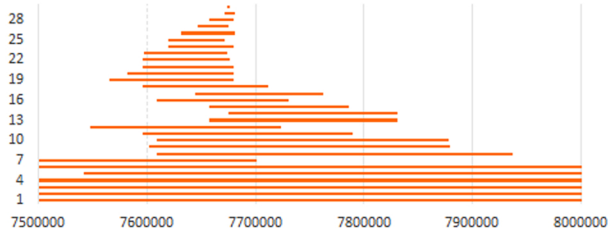

MAP2K4

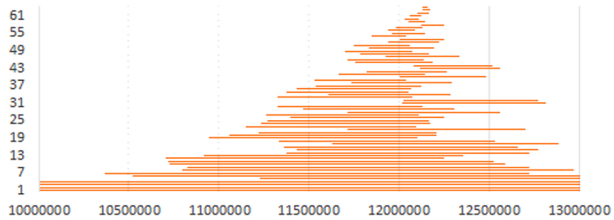

NF1

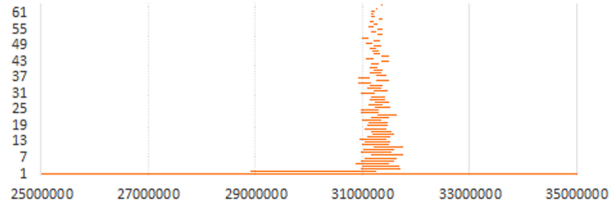

PTEN

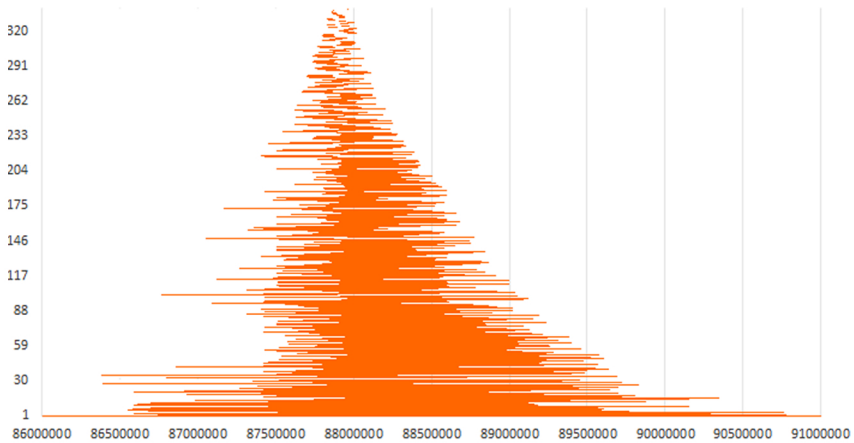

TGFBR2

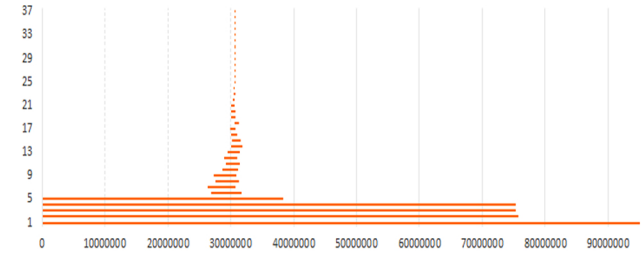

RB1

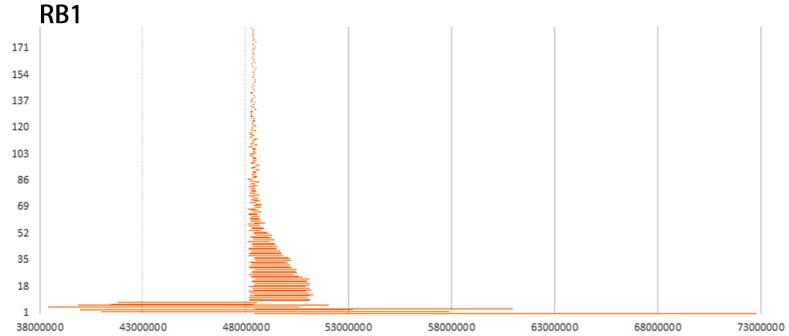

SMAD4

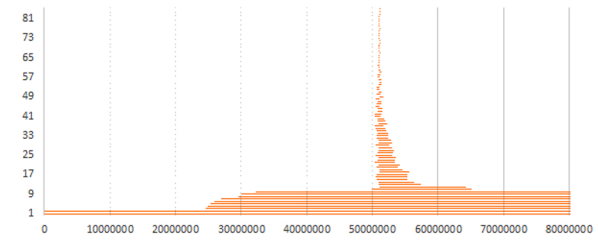

	TP53	MAP2K	NF1	RB1	SMAD4	PTEN	TGFBR2
Skewness	6.551	8.924	5.554	-.013	-.757	1.958	1.958
Std. Error of Skewness	.309	.214	.214	.127	.186	.094	.279
Kurtosis	47.298	94.979	77.258	-1.991	8.735	15.658	5.225
Std. Error of Kurtosis	.608	.425	.425	.253	.370	.187	.552